Journal of Advanced Research in Science and Technology
ISSN: 2352-9989

Effect of internal erosion (suffusion) on dikes stability: Finite element analysis

Abderrezak Bouziane [1*]

[1] Laboratoire de génie de la construction et d'architecture (LGCA), Faculté de Technologie, Université de Bejaia, 06000 Bejaia, Algérie

Abstract. In the present study a numerical solution is proposed in order to quantify the impact of internal erosion on dike stability. The mathematical model, consisting of erosion equations, mixture flow equations and stress equilibrium equations, is solved numerically by the finite element method using COMSOL MULTIPHYSICS software. The shear strength reduction technique is used to analyze the stability of a dike taking into account the effect of internal erosion. The variation in time and space of porosity, as internal erosion progresses, is chosen as a coupling parameter. We have considered that elasticity and soil resistance (cohesion) depend on porosity so that the material becomes weaker as porosity increases. The results show that the porosity increases significantly at the dike toe, which was explained by an erosion of this zone. Erosion at the dike toe induces alterations in the mechanical behavior of the medium. Since cohesion decreases with increasing porosity, the factor of safety of the downstream slope undergoes a significant modification. This study may help to better understand the phenomenon of internal erosion in dikes and to better prevent the stability of a hydraulic structure.

Keywords: *Internal erosion, Slope stability, Factor of Safety, Finite elements method*

1. Introduction

According to [1]–[3], 46% of the disorders observed on earthworks originate from internal erosion. Therefore, it is crucial to gain a fundamental understanding of the triggering mechanism and the process of internal erosion. In the literature, four types of processes are distinguished, namely: concentrated leak erosion, backward erosion, contact erosion or suffusion. To study the process of internal erosion of soils, various experimental studies have been proposed in the literature that rely mainly on the application of an infiltration flow through the soil sample, under a controlled hydraulic gradient and on the measurement of the amount of loose particles [4]–[8]. Numerical models of internal erosion are based on the theory of porous media, where the internal erosion of the soil skeleton and the transport of fine particles in the interstitial water are modeled by a mass exchange between the soil skeleton and interstitial water [9]–[12].

As far as the global instability is concerned, the slope stability analysis has been reported by several researchers, where it has been presented the different methods namely: the limit equilibrium method [13], the finite element method [14] and the boundary element method [15]. In the methods mentioned above, the stability of the slope is evaluated by the calculation of the safety factor (FOS) defined as the ratio of the resistance force to the driving force on the potential sliding surface; when the safety factor is greater than unity, the slope is considered stable.

* Corresponding author.
E-mail: a.bouziane.doc@gmail.com (Bouziane A.).
Address: Targa Ouzemmour, Bejaia 06000 Algeria

The problem of slope stability is further complicated by the presence of infiltration, erosion and headcutting caused by surface water. Infiltration, in particular, is often poorly represented in numerical models. Therefore, its erosive power is completely neglected. It is therefore crucial to establish an accurate prediction of the soil slope stability model under infiltration conditions.

In this paper we are interested in suffusion when the transport is diffused through the solid matrix and only concerns suspended fines. This phenomenon is widely detected in both natural deposits and charged structures. This is the process by which fine particles in the soil gradually migrate through the voids between coarse particles, leaving behind the skeleton of the soil. This study highlighted the effect of internal erosion on the change in soil resistance and its effect on the global stability of a soil structure. We try to do this bay relating the overall stability of the system to an internal parameter which is porosity.

First, we present the mathematical model of the erosion kinetics, based on considerations of mass balance and particle transport. The differential equations used to model mass transfer in porous media are those proposed by [16]. Next, we expose the Darcy flow equations with permeability that depends on porosity. The process of fluid flow and erosion coupled with mechanical damage is solved numerically by the finite element method using the COMSOL Multiphysics numerical modeling tool. An analysis of the stability of a dike by the shear strength reduction method is discussed in the second part of the study in order to show the effect of internal erosion (suffusion) on the stability of a slope.

2. Mathematical model of internal erosion

2.1.Definition

The saturated porous media is modeled as a three-phase system consisting of skeletal solids (s), fluidized solids (fs) and fluid (f) as shown in (Fig. 1). Fluidized particles are suspended particles that move with the fluid. All other free particles that are trapped within the void space are considered part of the solid phase. In addition, it is assumed that fluid and fluidized particles share the same speed at all times. The solid is supposed to be rigid. In other words, a solid particle has zero velocity and is assigned to the solid phase or fluid velocity and is assigned to the mixture that fills the void space. The volume fraction of the voids is expressed by the overall porosity.

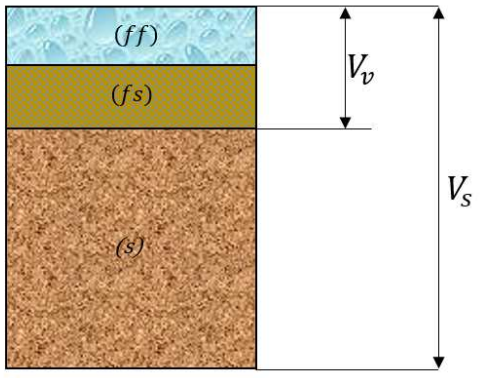

Figure 1: Phase diagram of porous medium saturated with fluid and fluidized particles

2.2.Mass balance equations

According to (Vardoulakis et al. 1996) [16], the equilibrium equation of fluidized solid particles (Eq.1) is expressed by

$$\frac{\partial(cn)}{\partial t} = q\nabla c + \frac{\partial n}{\partial t} \tag{1}$$

With

c : The concentration of the fluidized solid.

n : Porosity

q : The volumetric discharge rate; with $q = n * v$.

Where v is the DARCY's velocity.

The evolution law of the porosity is given by

$$\frac{\partial n}{\partial t} = \lambda(1-n)cq \tag{2}$$

With

$\boldsymbol{\lambda}$: Coefficient probably related to the spatial frequency of the trigger points of the erosion potential in the solid skeletal of the porous medium. Its dimension is the inverse of length, $[\boldsymbol{\lambda}] = \boldsymbol{L^{-1}}$.

2.3.Constitutive laws of mass generation

Extensive experimental and theoretical studies on the filtration of non-colloidal solid particles in porous media were conducted in the late 60's by H. A. Einstein of the University of California at Berkeley. This work, summarized in the articles by [18] and [19], resulted in a constitutive equation that governs the kinetics of filtration. These ideas are adopted here in the form of a simple constitutive law for the eroded mass ratio given by

$$\dot{m} = \rho_s \lambda \frac{1-n}{k} c \|\bar{q}_i\| \tag{3}$$

2.4.DARCY's flow in a porous medium

Fluid flow in this problem can be described using Darcy's law

$$\frac{\partial n\rho_f}{\partial t} + \nabla.\rho_f u = 0 \tag{4}$$

$$u = -\frac{k}{\mu}(\nabla p + \rho_f g \nabla H) \tag{5}$$

Here, ρ_f is the water density (kg/m^3), t is the time (s), n is the porosity and u is the Darcy's velocity. Darcy's speed depends on the permeability $k\ (m^2)$, the dynamic viscosity of the fluid $\mu\ (Pa.s)$, fluid pressure $p\ (Pa)$ and the gravity acceleration $g\ (m/s^2)$. Elevation gradient $H\ (m)$ indicates the direction of the vertical coordinate, y.

Changes in porosity affect significantly the permeability of the medium. We remember that the physical permeability k of a porous medium depends on the porosity. For example, according to the Carman-Kozeny equation (Eq.4). On the other hand, permeability enters the problem of fluid flow through Darcy's law.

$$k = k_0 \frac{n^3}{(1-n)^2} \tag{6}$$

We remember that Darcy's law derives from (a) the equilibrium of motion for the fluid phase and (b) from a constitutive equation of the fluid-solid interaction force (that is, the force of infiltration).

Thus, in a process where the porosity varies locally over time due to erosion, the fluid flow in the pore space becomes a nonlinear phenomenon controlled by particle erosion. The viscosity of the fluid μ is formally a function of the density of the fluid-particle mixture given by [16], [20]

$$\bar{\rho} = (1-c)\rho_f + c\rho_s \tag{7}$$

With

$\bar{\rho}$: the apparent density of the soil

ρ_f : the fluid density

ρ_s : grains density

However, the analysis of the sand production problem shows that the changes in the concentration c of the fluidized particles are small and that, consequently, the density $\bar{\rho}$ remains essentially constant during the erosion process [16]. Thus, a constant viscosity of the fluid has been adopted to model the sand production process. [21]. This restriction can, however, be relaxed in problems where changes in concentration become important.

3. Slope stability analysis

The erosion phenomena in turn cause degradation of the granular medium by increasing the porosity and decreasing the cohesion between the grains. The degradation of the medium is described by a simple law of damage according to which the decrease of the cohesion $\bar{C}$ is quantitatively proportional to the porosity [21].

$$\bar{C} = \bar{\bar{C}} \frac{1-n}{1-n_0} \tag{8}$$

according to [21], we introduce the running Young modulus defined by

$$E = \bar{\bar{E}} \frac{1-n}{1-n_0} \tag{9}$$

4. Application on a dike

In this part, a dike whose geometry is shown in Figure 1 is considered as an example of application. The soil constituting the dike is considered homogeneous.

4.1.Geometry of the dike

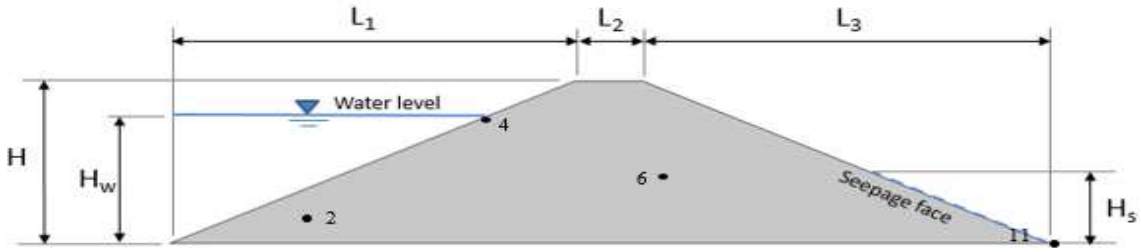

Figure 2: Geometry of the dike

With

$$L1 = L3 = 24\ m, L2 = 5\ m, H = 12\ m, Hw = 10\ m, Hs = 4\ m.$$

4.2.Erosion model parameters

The calculation results for the erosion and dike stability problem will be presented for all the parameters presented in Table 1. With these data, the process starts at the moment $t = 0$ of a Darcy flow.

Table 1: Input parameters of the calculation example

Parameter	Value
Initial porosity	$n = 0.4$
Initial concentration	$c_0 = 0$
Initial permeability	$k0 = 1.0228 \times 10^{-11}\ m^2$
Dynamic viscosity	$\mu = 0.001002\ Pa.s$
Water density	$\rho_f = 1000\ kg/m^3$
Grains density	$\rho_s = 2700\ kg/m^3$
Young modulus	$E = 10^5 kN/m^2$
Cohesion	$C = 25\ kPa$
Internal friction angle	$\varphi = 30°$
Upstream pressure head	$H = 10\ m$

4.3.Domain mesh

The extremely fine mesh is free triangles type with an automatic method. This type of mesh has been applied after preliminary numerical tests of the accuracy of the calculation. The final mesh consists of 3250 triangular elements. Figure 2 shows the mesh chosen for the entire domain.

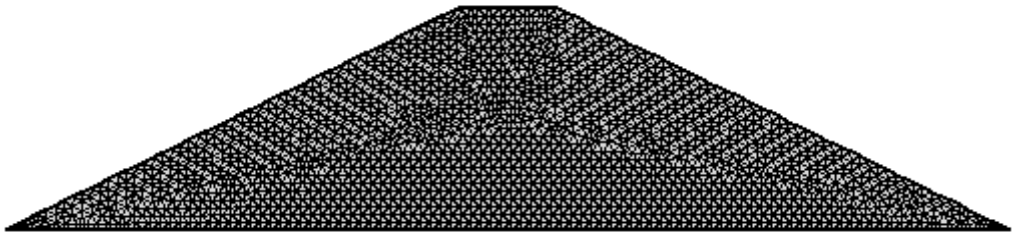

Figure 3: The extremely fine mesh of the model

5. Results and discussions

In this section, we present the results of suffusion modeling in earthworks conducted by the COMSOL Multiphysics software. The soil is treated as an elasto-plastic Mohr-Coulomb solid infiltrated with fluid governed by Darcy's law. The modeling was performed considering the parameters presented in Table 1.

FIG. 9a shows the temporal variation of permeability at the dike toe. It can be seen that the permeability increase significantly. Takahashi [22] argued that the type of failure essentially depends on dam permeability and material strength. In the case of very high permeability, failure is due to headcutting migrating upstream after toe erosion of the downstream face as can be seen in (Fig. 7a) which shows a loss of the cohesion of the material. This latter mechanism is also observed by both laboratory experiments [23]–[26] and field observations [25], [27]–[29]. The surface flow that occurs on the dike downstream face, beneath the phreatic surface exit, is responsible for the removal of surficial layer grains and formation and migration of the headcutting erosion channel [30].

In FIG. 4, using Darcy's law mode in Comsol, we present flow velocity mapping (u) with the velocity field through the medium for (t = 1000 d). the speed range of the flow indicated in FIG. 1.b is widely variable between 0 and 10 * 104 m/s at the end of calculation.

The porosity evolution (n), the Young's modulus (E), the cohesion (C) and the concentration (c) at the various points of the medium, are respectively shown in FIGS. 5, 6, 7 and 8.

In FIG. 5, the point (11) near the upstream, the point (4) near the downstream are in areas where the porosity has undergone a significant increase. This increase can be expressed by a significant erosion of these areas which leads to the loss of cohesion of the material as shown in FIG. 7.

In Fig.5b, the point (11) near the upstream, the point (4) near the downstream are in areas where the porosity has undergone a significant increase. This increase can be expressed by a significant erosion of these areas which leads to the loss of cohesion of the material as shown in Fig.7b.

The erosion of the dike toe explained by the high increase in porosity at this location (water infiltration zone) as shown in Fig.5b is in good agreement with the experience of [32][20][33].

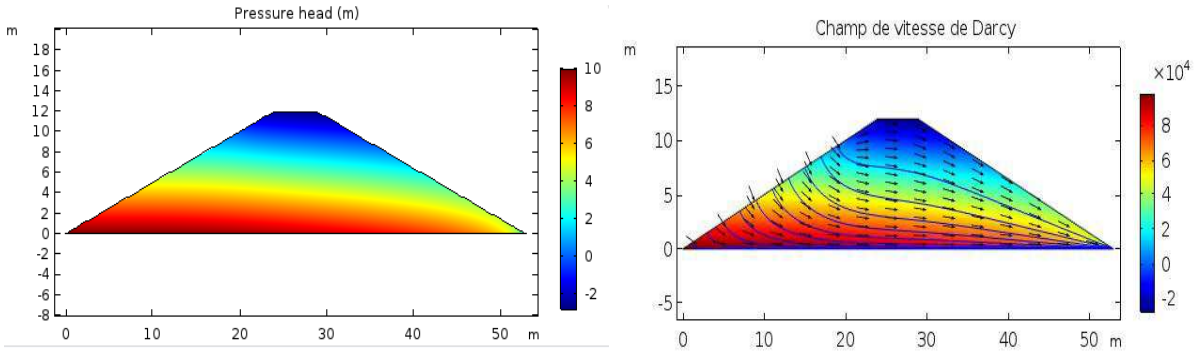

(a) (b)

Figure 4: (a) Pressure head mapping, (b) Darcy's velocity fields

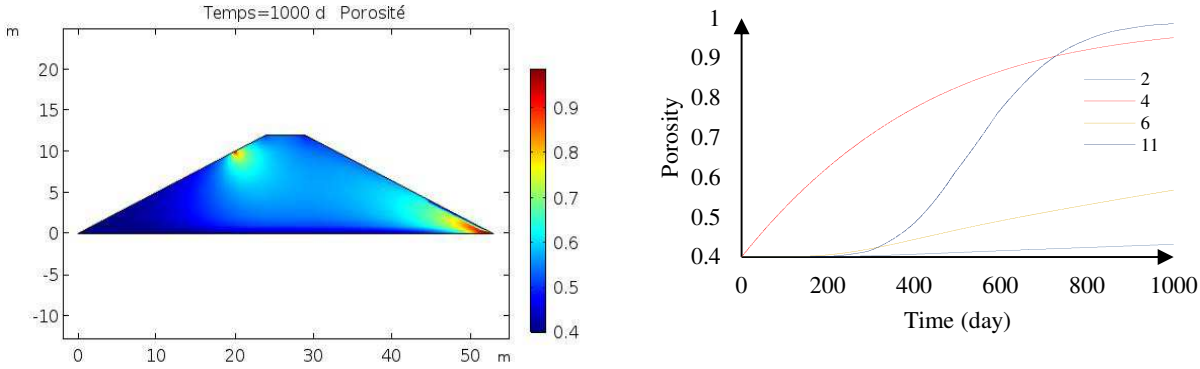

(a) (b)

Figure 5: (a) The spatial distribution of the porosity at time t = 1000 d, (b) Temporal variation of porosity at different locations on the dike

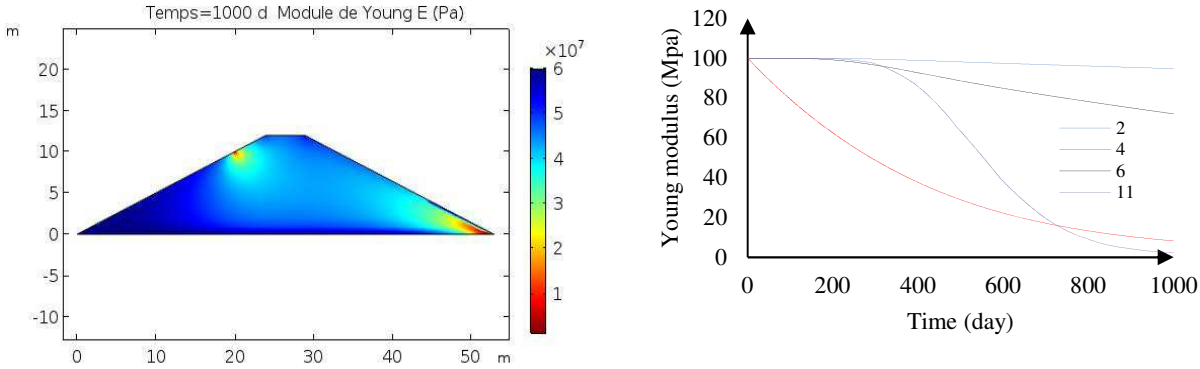

(a) (b)

Figure 6: (a) The spatial distribution of Young modulus at time t = 1000 d (b) Temporal variation of the Young

modulus at different locations on the dike

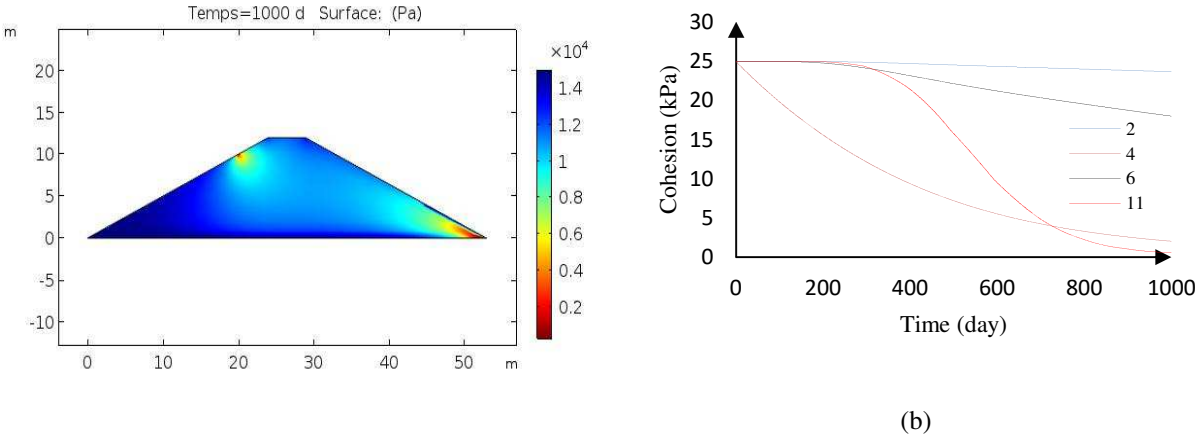

(a) (b)

Figure 7: (a) The spatial distribution of cohesion at time t = 1000 d, (b) Temporal variation of cohesion at different locations in the dike

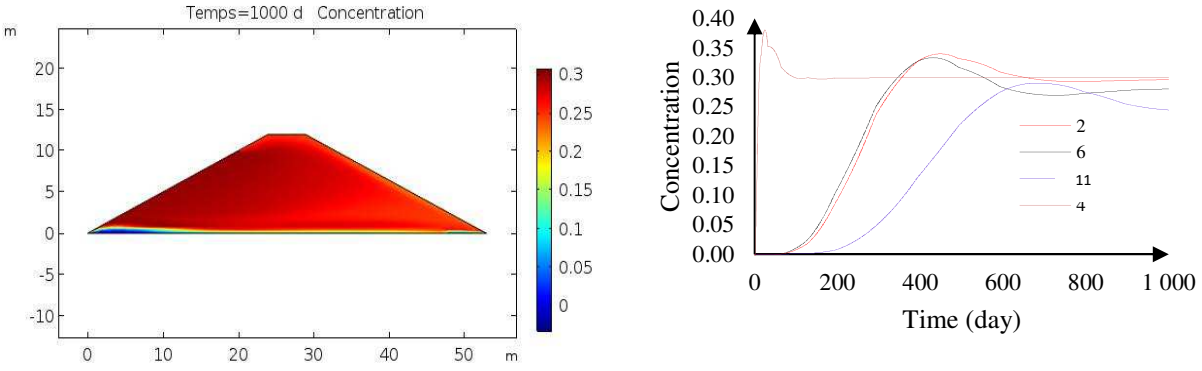

(a) (b)

Figure 8: (a) The spatial distribution of concentration at time t = 1000 d, (b) Temporal variation of concentration at different locations in the dike

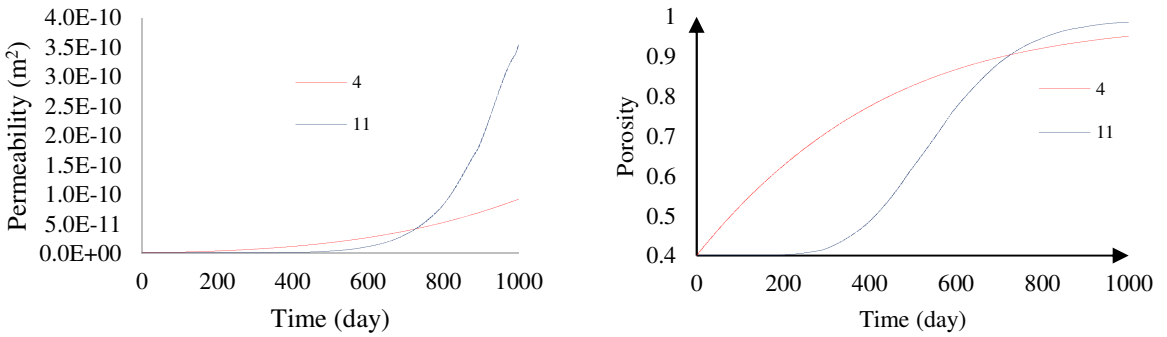

(a) (b)

Figure 9: Temporal variation of permeability at upstream and downstream, (b) Temporal variation of porosity at upstream and downstream

6. Slope stability

As far as the global instability is concerned, the soil resistance parameters are taken in the area where the sliding surface is potential (FIG. 1: point 6) and at time intervals of 250 days. The parameters considered in this section are summarized in Table 2. For each measuring point the stability analysis is carried out and the safety factor and the maximum displacement are determined. FIG. 10a shows the potential sliding surface at the final phase of erosion. FIG. 10b shows the temporal variation of the safety factor due to erosion. These results highlight the effect of erosion on the stability of an earth structure where stability is reduced by about 16%.

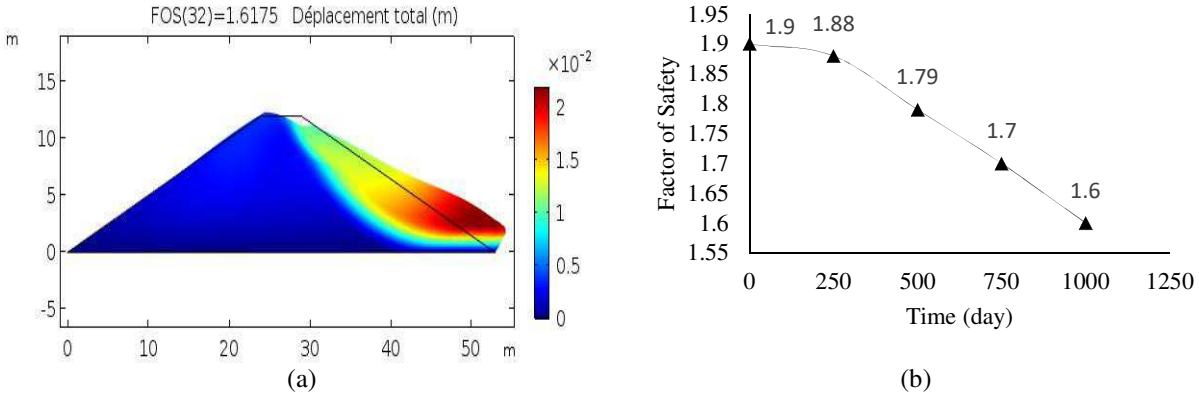

Figure 10: (a) Sliding surface at the final phase of erosion, (b) Variation of the safety factor due to internal erosion

Table 2: Variation of parameters over time due to internal erosion (point 6)

$Time\ (day)$	$C\ (kPa)$	$E\ (MPa)$	FOS	$U_{max}(cm)$
0	25	100	1.9	1.80
250	24.5	98	1.88	2.00
500	22	88	1.79	2.22
750	20	79.8	1.7	2.33
1000	18	75	1.6	2.50

7. Conclusion

This article presents a study of the influence of internal erosion (suffusion) in a dike on its mechanical behavior. The variation in time and space of porosity, as internal erosion progresses, is chosen as a coupling parameter. We have considered that elasticity and soil resistance (cohesion) depend on porosity so that the material becomes weaker as porosity increases. The mathematical model, composed of erosion equations, mixture flow equations and stress equilibrium equations is solved numerically by the finite element method. The analysis of the obtained results made it possible to draw the following conclusions:

- The erosion of the dike toe explained by the high increase in porosity at this location (water infiltration zone) is in good agreement with the experience of [32] [20] [33].

- Erosion near the free surface is accompanied by a significant increase in permeability.
- In addition, the increase in porosity results in a reduction of the cohesion between the grains and a reduction of the rupture envelope.
- Erosion at the dike toe induces alterations in the mechanical behavior of the environment. Since cohesion decreases with increasing porosity, the moment dike begins to break may be identified.
- We found that erosion causes a significant change in slope stability and should be included in the modeling of this problem.
- Erosion at the toe of the downstream slope of the dike is captured by comparing initial and final cohesion. The total loss of cohesion leads to the loss of shear strength.

The results of the study indicate that experimental research would be needed to determine the erosion parameter (lambda), validate the model and to better understand the different aspects of the problem, especially those related to changes in mechanical properties of soil subjected to erosion. In addition to variations in stiffness and shear strength, the influence of fines content on soil expansion and post erosion behavior could also be investigated.

8. References

[1] M. Foster, R. Fell, and M. Spannagle, "The statistics of embankment dam failures and accidents," *Can. Geotech. J.*, vol. 37, no. 1992, pp. 1000–1024, 2000.

[2] C. F. Wan and R. Fell, "Experimental investigation of internal stability of soils in embankment dams and their foundation," UNICIV report ; no. R-429, University of New South Wales, Sydney, Australia, 2004.

[3] J. Zhang, L. I. Yun, X. Guoxiang, W. Xiaogang, and L. I. Jun, "Overtopping breaching of cohesive homogeneous earth dam with different cohesive strength," vol. 52, no. 10, 2009.

[4] T. Hadj-Hamou, M. R. Tavassoli, and W. C. Sherman, "LABORATORY TESTING OF FILTERS AND SLOT SIZES FOR RELIEF WELLS," vol. 116, no. 9, pp. 1325–1346, 1991.

[5] T. C. Kenney and D. Lau, "Internal stability of granular filters," *Can. Geotech. J.*, vol. 22, no. 2, pp. 215–225, May 1985.

[6] M. Ouyang and A. Takahashi, "Influence of initial fines content on fabric of soils subjected to internal erosion," *Can. Geotech. J.*, vol. 15, no. JANUARY, pp. 1–15, 2015.

[7] D. Sterpi, "Effects of the Erosion and Transport of Fine Particles due to Seepage Flow," *Int. J. Geomech.*, vol. 4, no. September, pp. 191–198, 2003.

[8] K. R. Reddy and K. S. Richards, "Experimental investigation of initiation of backward erosion piping in soils," *Géotechnique*, vol. 62, no. 10, pp. 933–942, 2012.

[9] A. Cividini and G. Gioda, "Finite-element approach to the erosion and transport of fine particles in granular soils," *Int. J. Geomech.*, vol. 4, no. September, pp. 191–198, 2004.

[10] R. S. Govindaraju, "Non-dimensional analysis of a physically based rainfall-runoff-erosion model over steep slopes," *Sediment. Geol.*, vol. 22, no. 3–4, pp. 165–184, 1994.

[11] A. Chetti, A. Benamar, and A. Hazzab, "Modeling of Particle Migration in Porous Media: Application to Soil Suffusion," *Transp. Porous Media*, vol. 113, no. 3, pp. 591–606, 2016.

[12] A. Benamar and A. Seghir, "PHYSICAL AND ANALYTICAL MODELING OF INTERNAL EROSION OF FINE PARTICLES IN COHESIONLESS SOILS," *J. Porous Media*, vol. 20, no. 3, pp. 205–216, 2017.

[13] J. M. Duncan, "State of the Art: Limit Equilibrium and Finite-Element Analysis of Slopes," *J. Geotech. Eng.*, vol. 122, no. 7, pp. 577–596, 1996.

[14] T. Matsui and K.-C. San, "Finit element slope stability analysis by shear strength reduction technique," *Japanese Soc. soil Mech. Found. Eng.*, vol. 32, no. 1, pp. 59–70, 1992.

[15] Y. Jiang, *Slope analysis using boundary elements*, vol. 52. New York: Springer-Verlag, 1990.

[16] I. Vardoulakis, M. Stavropoulou, and P. Papanastasiou, "Hydro-mechanical aspects of the sand

production problem," *Transp. Porous Media*, vol. 22, no. 2, pp. 225–244, 1996.
[17] H. A. Einstein, "Der Geschiebetrieb als Wahrscheinlichkeitsproblem," ETH Zürich, 1936.
[18] R. Sakthivadivel and S. Irmay, "A review of filtration theories," Berkeley, Calif.: Hydraulic Engineering Laboratory, College of Engineering, University of California, Berkeley., 1966.
[19] R. Sakthivadivel, *Theory and mechanism of filtration of non-colloidal fines through a porous medium*. 1967.
[20] M. Stavropoulou, P. Papanastasiou, and I. Vardoulakis, "Coupled wellbore erosion and stability analysis," *Int. J. Numer. Anal. Methods Geomech.*, vol. 22, no. 9, pp. 749–769, 1998.
[21] E. Gravanis, E. Sarris, and P. Papanastasiou, "Volumetric sand production model and experiment," *Int. J. Numer. Anal. Methods Geomech.*, vol. 25, no. 8, pp. 789–808, Jul. 2001.
[22] T. Takahashi, "A Review of Japanese Debris Flow Research," *Int. J. Eros. Control Eng.*, vol. 2, no. 1, pp. 1–14, 2007.
[23] M. J. Franca and A. B. Almeida, "Experimental Tests on Rockfill Dam Breaching Process," *IAHR - Int. Symp. Hydraul. Hydrol. Asp. Reliab. Saf. Assess. Hydraul. Struct.*, 2002.
[24] W. M. Liao and H. T. Chou, "Debris flows generated by seepage failure of landslide dams," no. 2000, p. 77017, 2003.
[25] A. Wörman, "Seepage-Induced Mass Wasting in COARSE SOIL SLOPES," vol. 119, no. 10, pp. 1155–1168, 1993.
[26] M. Y. F. Huang, H. Capart, R. Chen, and A. Y. L. Huang, *Experimental analysis of the seepage failure of a sand slope*. Rotterdam, The Netherlands: Proc., 4th Int. DFHM Conf., C. Chen and J. J. Major, eds., Millpress, 2007.
[27] D. M. Cruden, T. R. Keegan, and S. Thomson, "The landslide dam on the Saddle River near Rycroft, Alberta," *Can. Geotech. J.*, vol. 30, no. 25, pp. 1003–1015, 1993.
[28] T. Leps, "Flow Through Rockfill," *Embankment-Dam Eng.*, pp. 87–107, 1973.
[29] W. Meyer, R. L. Schuster, Fellow, ASCE, and M. A. Sabol, "Potential for seepage erosion of landslide dam," vol. 120, no. 7, pp. 1211–1229, 1994.
[30] C. Gregoretti, A. Maltauro, and S. Lanzoni, "Laboratory Experiments on the Failure of Coarse Homogeneous Sediment Natural Dams on a Sloping Bed," *J. Hydraul. Eng.*, vol. 136, no. 11, pp. 868–879, 2010.